A Hole-Attractor Model: Tailoring Manganese-Related Perovskites

José M. Alonso,[†,‡] Alfredo Arroyo,[†] José M. González-Calbet,*[,§] Antonio Hernando,[†,||] Juan M. Rojo,[||] and María Vallet-Regí[⊥]

Instituto de Magnetismo Aplicado, UCM-CSIC-RENFE, Las Rozas, P.O. Box 155, Madrid 28230, Spain, Instituto de Ciencia de Materiales (ICMM), CSIC, Cantoblanco, 28049 Madrid, Spain, Departamento de Química Inorgánica, Facultad de Químicas, Universidad Complutense, 28040 Madrid, Spain, Departamento de Física de Materiales, Facultad de Físicas, Universidad Complutense, 28040 Madrid, Spain, and Departamento de Química Inorgánica y Bioinorgánica, Facultad de Farmacia, Universidad Complutense, 28040 Madrid, Spain

Received May 14, 2003
Revised Manuscript Received June 6, 2003

Understanding the phase diagrams of hole-doped lanthanum manganese perovskites of general formula $(La_{1-x}Ca_x)_{1-z}Mn_{1-y}O_{3-\delta}$ is a matter of current interest in view of the still largely unexplained electric and magnetic properties of these compounds.[1] The double-exchange mechanism, proposed by Zener,[2] accounts for the metallic and ferromagnetic behavior of these oxides but is insufficient to describe their high-temperature transport properties, to quantify their large-resistance drop, or to explain the complexity of their magnetic and electric phase diagrams.[3,4] The so-called phase separation (PS) model proposes the coexistence of two types of nanometer-size clusters corresponding to a ferromagnetic-metallic (FM-C) phase and a correlated-insulating (I) one. The latter involves a charge-ordered (CO) state characterized by an ordered array of holes (Mn^{4+}) in every other Mn ion dominated by Coulomb interactions.[5] The PS model is in reasonable agreement with numerous experimental results,[6] which reveal a great complexity of phases involving different electric and magnetic states, for example, those included in the phase diagrams.[3,4] However, recent results have proved[7,8] that, in addition to providing holes to the band, the divalent substituting ions act as effective attractors for these holes. This effect is not accounted for in the standard PS model and an extension of the latter is needed.

In most of the previous work in these mixed-valence compounds, hole doping is induced by the substitution of a rare-earth ion (e.g., La) by an alkaline-earth divalent ion (e.g., Ca), every substituted Ca ion creating a hole (h^+) in the e_g Mn levels. Unfortunately, only in rare cases is the alternative mechanism of hole creation, through the generation of cationic vacancies, controlled and, practically, never taken into account in the theoretical models. In this report, by controlling the cationic vacancies as a means of governing the concentration of Mn^{4+} holes, n_h, *independently* of the divalent atom concentration, x, we report experimental results which give support to a simple model describing the double role of substitutional Ca ions.

Cationic-deficient manganese perovskites have been prepared following the recipes and taking the precautions of earlier investigations.[7,9−11] Our air-synthesized perovskites have always been prepared at 1400 °C with $0 < z < 0.1$. In the low Ca doping region, the concentrations of Mn vacancies are always lower than 4.5%. The second column of Table 1 shows the chemical composition of all samples according to inductive coupling plasma, energy dispersive spectroscopy, and thermogravimetric analysis.

For temperatures *below* T_c, above which holes are excited, the electrical and magnetic characteristics of our samples together with those of earlier work[7,8] are summarized in the third to sixth columns of Table 1. An example of the raw curves from which these characteristics are derived is shown as Figure 1. The model we propose is based on two assumptions. (i) Divalent substitutional ions act as hole attractors, resulting in hole aggregates around Ca ions. This is consistent with the well-known fact that $CaMnO_3$, in which all the Mn in the Mn^{4+} hole configuration are structural units with a high degree of stability. (ii) The formation and/or stabilization of clusters of the correlated CO phase requires the presence of nuclei involving a minimum number of neighboring Ca ions. This second assumption is in agreement with recent data of Kiryukhin et al.,[12] showing that the CO phase consists of small clusters and that, at $x = 0.5$, most of the sample is in the correlated phase whereas only a small fraction is so at $x = 0.3$.

We assume that three is the minimum Ca content for a nucleus in the correlated phase. Then, the fraction of Ca ions in correlated clusters, x_1, will be proportional to x^3, that is,

$$x_1 = Cx^3 \tag{1}$$

where C is a constant. Measurements in related systems

* To whom correspondence should be addressed.
† Instituto de Magnetismo Aplicado, UCM-CSIC-RENFE.
‡ Instituto de Ciencia de Materiales (ICMM), CSIC.
§ Facultad de Químicas, Universidad Complutense.
|| Facultad de Físicas, Universidad Complutense.
⊥ Facultad de Farmacia, Universidad Complutense.

(1) Salamon, M. B.; Jaime, M. *Rev. Mod. Phys.* **2001**, *73*, 583.
(2) Zener, C. *Phys. Rev.* **1951**, *82*, 403.
(3) Cheong, S. W.; Hwang, H. Y. In *Colossal Magnetoresistive Oxides Monographs In Condensed Matter Science*; Tokura, Y., Ed.; Gordon & Breach: Reading, UK, 2000; Chapter 7.
(4) Schiffer, P.; Ramirez, A. P.; Bao, W.; Cheong, S. W. *Phys. Rev. Lett.* **1995**, *75*, 3336.
(5) Moreo, A.; Yunoki, S.; Dagotto, E. *Science* **1999**, *283*, 2034.
(6) Fath, M.; Freisem, S.; Menovsky, A. A.; Tomioka, Y.; Aarts, J.; Mydosh, J. A. *Science* **1999**, *285*, 1540.
(7) Alonso, J.; Herrero, E.; González-Calbet, J. M.; Vallet-Regí, M.; Martínez, J. L.; Rojo, J. M.; Hernando, A. *Phys. Rev. B* **2000**, *62*, 11328.
(8) Alonso, J.; Arroyo, A.; González-Calbet, J. M.; Vallet-Regí, M.; Martínez, J. L.; Rojo, J. M.; Hernando, A. *Phys. Rev. B* **2001**, *64*, 172410.
(9) Majewski, P.; Epple, L.; Rozumek, M.; Schluckwerder, H.; Aldinger, F. *J. Mater. Res.* **2000**, *15* (5), 1161.
(10) Mahesh, R.; Kannan, R. K.; Rao, C. N. R. *J. Solid State Chem.* **1995**, *114*, 294.
(11) Joy, P. A.; Raj Sankar, C.; Date, S. K. *J. Phys.: Condens. Matter* **2002**, *14*, L663.
(12) Kiryukhin, V.; Koo, T. Y.; Borissov, A.; Kim, Y. J.; Nelson, C. S.; Hill, J. P.; Gibbs, D.; Cheong, S. W. *Phys. Rev. B* **2002**, *65*, 094421.

10.1021/cm0343599 CCC: $25.00
Published on Web 07/03/2003

Table 1. Chemical Composition and Magnetic and Electrical Properties for Samples $(La_{1-x}Ca_x)_{1-z}Mn_{1-y}O_{3-\delta}$[a]

	experimental data					calculated values			
first	second	third	fourth	fifth	sixth	seventh	eighth	ninth	tenth
sample	composition (measured)	x	n_h	magnetic[b]	electric	x_1	$x - x_1$	$1 - 2x_1$	q_2
$A_{0.00}$	$La_{0.96}(Mn^{4+}_{0.18}Mn^{3+}_{0.82})_{0.96}O_{2.97}$	0	0.18	FM/AF	C	0	0	1	0
this work	$(La_{0.98}Ca_{0.02})_{0.96}(Mn^{4+}_{0.05}Mn^{3+}_{0.95})_{0.96}O_{2.89}$	0.02	0.05	SP	I	≈0	0.02	1	0.02
$A_{0.05}$	$(La_{0.95}Ca_{0.05})_{0.96}(Mn^{4+}_{0.09}Mn^{3+}_{0.91})_{0.96}O_{2.90}$	0.05	0.09	FM/AF	I	≈0	0.05	1	0.05
$A_{0.10}$	$(La_{0.90}Ca_{0.10})_{0.97}(Mn^{4+}_{0.14}Mn^{3+}_{0.86})_{0.97}O_{2.93}$	0.10	0.14	FM/AF	I	≈0	0.10	1	0.10
$A_{0.20}$	$(La_{0.80}Ca_{0.20})_{0.99}(Mn^{4+}_{0.24}Mn^{3+}_{0.76})_{0.99}O_{2.99}$	0.20	0.24	FM	C	0.03	0.17	0.94	0.18
$A_{0.25}$	$(La_{0.75}Ca_{0.25})(Mn^{4+}_{0.25}Mn^{3+}_{0.75})O_{2.99}$	0.25	0.25	FM	C	0.06	0.17	0.88	0.19
$O_{0.00}$	$La_{0.96}(Mn^{4+}_{0.25}Mn^{3+}_{0.75})_{0.96}O_{3.00}$	0	0.25	FM	C	0	0	1	0
$O_{0.05}$	$(La_{0.95}Ca_{0.05})_{0.96}(Mn^{4+}_{0.29}Mn^{3+}_{0.71})_{0.96}O_{3.00}$	0.05	0.29	FM	I	≈0	0.05	1	0.05
$O_{0.10}$	$(La_{0.90}Ca_{0.10})_{0.97}(Mn^{4+}_{0.28}Mn^{3+}_{0.72})_{0.97}O_{3.00}$	0.10	0.28	FM	I	≈0	0.10	1	0.10
$O_{0.20}$	$(La_{0.80}Ca_{0.20})_{0.99}(Mn^{4+}_{0.27}Mn^{3+}_{0.73})_{0.99}O_{3.00}$	0.20	0.27	FM	C	0.03	0.17	0.94	0.18
$O_{0.25}$	$(La_{0.75}Ca_{0.25})(Mn^{4+}_{0.27}Mn^{3+}_{0.73})O_{3.00}$	0.25	0.27	FM	C	0.06	0.19	0.88	0.22
Ia[c]	$La_{0.50}Ca_{0.50}Mn^{4+}_{0.50}Mn^{3+}_{0.50}O_{3.00}$	0.50	0.50	AF	I	0.45	0.05	0.1	0.05
this work	$La_{0.52}Ca_{0.46}Mn^{4+}_{0.50}Mn^{3+}_{0.50}O_{3.00}$	0.46	0.50	SP/FM	I/C	0.35	0.11	0.3	0.37
Ib[c]	$La_{0.55}Ca_{0.43}Mn^{4+}_{0.50}Mn^{3+}_{0.50}O_{3.00}$	0.43	0.50	FM	C	0.29	0.14	0.42	0.33
Ic[c]	$La_{0.60}Ca_{0.35}Mn^{4+}_{0.50}Mn^{3+}_{0.50}O_{3.00}$	0.35	0.50	FM	C	0.15	0.20	0.7	0.29
Id[c]	$La_{0.65}Ca_{0.28}Mn^{4+}_{0.50}Mn^{3+}_{0.50}O_{3.00}$	0.28	0.50	FM	C	0.08	0.20	0.84	0.24
IIa[c]	$La_{0.50}Ca_{0.50}Mn^{4+}_{0.50}Mn^{3+}_{0.50}O_{3.00}$	0.50	0.50	AF	I	0.45	0.05	0.1	0.50
IIb[c]	$La_{0.50}Ca_{0.50}Mn^{4+}_{0.46}Mn^{3+}_{0.54}O_{2.98}$	0.50	0.46	AF	I	0.45	0.05	0.1	0.50
IIc[c]	$La_{0.50}Ca_{0.50}Mn^{4+}_{0.40}Mn^{3+}_{0.60}O_{2.95}$	0.50	0.40	AF	I	0.45	0.05	0.1	0.50
this work	$La_{0.60}Ca_{0.30}Mn^{4+}_{0.60}Mn^{3+}_{0.40}O_{3.00}$	0.30	0.60	FM	C	0.10	0.20	0.8	0.25
this work	$La_{0.43}Ca_{0.50}Mn^{4+}_{0.70}Mn^{3+}_{0.30}O_{3.00}$	0.50	0.70	AFM	I	0.45	0.05	0.1	0.50

[a] Calculated values are obtained from Eq. [1], [2] and [4]. [b] FM = ferromagnetic, AF = antiferromagnetic, and SP = superparamagnetic. [c] Data for samples A and O are from ref 7; the ones named Ia, Ib, etc. correspond to Table 1 and those named IIa, IIb, etc. to Table 2 of ref 8.

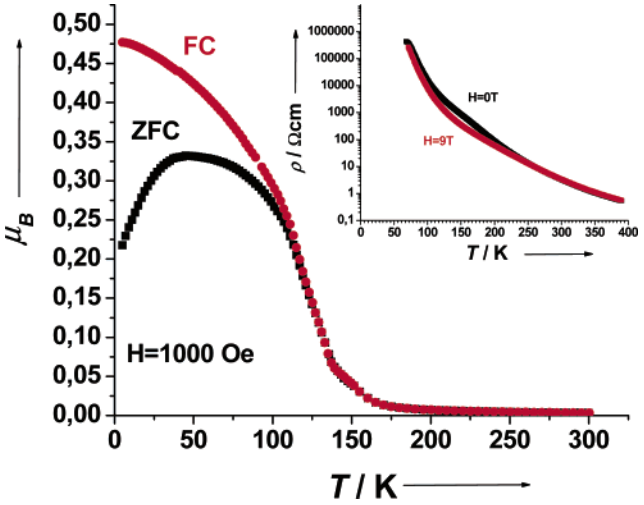

Figure 1. Thermal dependence of magnetization, under a 1000 Oe applied field, for a sample of $(La_{0.98}Ca_{0.02})_{0.96}(Mn^{4+}_{0.05}Mn^{3+}_{0.95})_{0.96}O_{2.89}$. Electrical resistance dependence is shown at the inset. This sample corresponds to the 2nd line of Table 1.

suggest[13] that, for $x = 0.50$, a fraction of about 10% of the volume remains in the FM-C phase. This leads to $C = 3.6$. A fraction x_1 of Ca ions in the CO phase occupies a fraction $2x_1$ of cationic positions because in the CO phase there is cationic disorder and, in the sublattice A, each Ca is, *on the average*, surrounded by La. The fraction of cationic positions "available" for the Ca ions in the uncorrelated phase will, then, be equal to $1-2x_1$ and the density of uncorrelated Ca ions, q_2:

$$q_2 = \frac{\text{number of uncorrelated Ca}}{\text{available cationic sites}} = \frac{x - x_1}{1 - 2x_1} = \frac{x - Cx^3}{1 - 2Cx^3} \quad (2)$$

The values of the four quantities x_1, $x - x_1$, $1 - 2x_1$, and q_2 are also included in Table 1 (columns 7−10). We check now the predictions of the model vs the experimental results.

In undoped samples trapping effects will be absent. Beyond the critical percolation concentration of h^+, $n_h = n_h^{crit}$, double exchange should result in FM-C behavior. For the simple-cubic arrangement of Mn positions, the theoretical lowest percolation value corresponds to a cubic cell whose side is twice as large as the initial one, that is, $n_h^{crit} \approx 0.125$. This agrees with our experimental evidence of a FM-C behavior for $n_h < 0.18$ (Table 1, samples $A_{0.00}$ and $O_{0.00}$) and Mahendiran's et al.,[14] which find an I-state for $n_h < 0.12$.

Samples with low doping appear electrically-I, even if the concentration of holes is higher than those in the FM-C undoped samples. These results cannot be explained either in terms of the simple double-exchange mechanism or in terms of the PS model. Yet they can be understood on the basis of our model by recalling that Ca ions act as very efficient traps for the h^+ (Mn^{4+}). One would not expect the onset of metallic-like conduction until the threshold of percolation *among the Ca* aggregates, $x = 0.125$, were reached, independently of the concentration of holes. Experimentally, one sees that samples become metallic for a threshold value of $0.10 > q_2 > 0.18$. This agrees indeed with the model that predicts this threshold at the onset of overlap among the Ca hole clusters when the average distance d between two Ca in the uncorrelated volume is equal to twice the distance a between cationic neighbors:

$$q_2 = \left(\frac{a}{d}\right)^3 > 0.125 \quad (3)$$

(13) Freitas, R. S.; Ghivelder, L.; Levy, P.; Parisi, F. *Phys. Rev. B* **2002**, *65*, 104403.
(14) Mahendiran, R.; Tiwary, S. K.; Raychaudhuri, A. K.; Ramakrishnan, T. V. *Phys. Rev. B* **1996**, *53*, 3348.

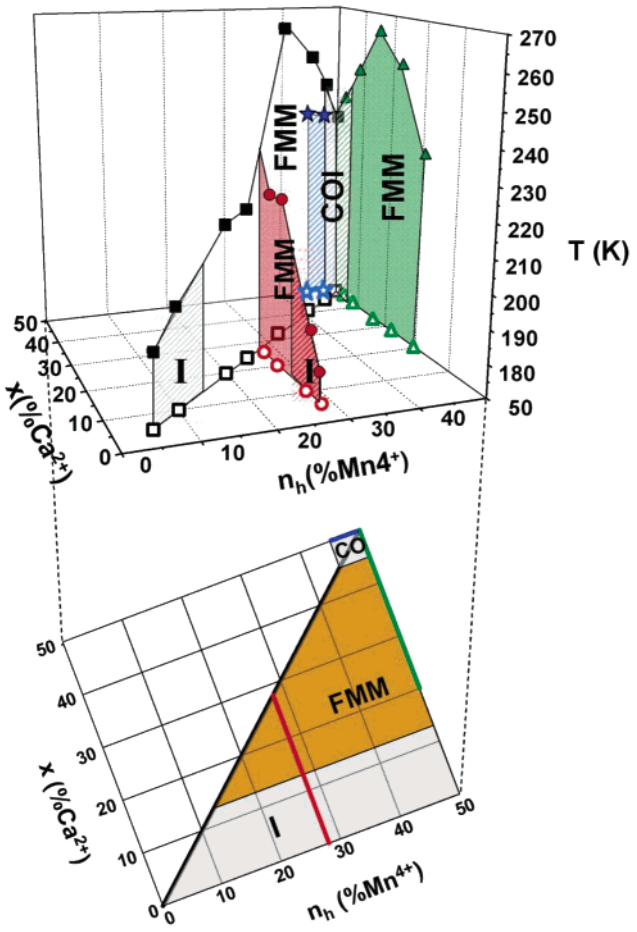

Figure 2. Magnetic and electrical three-dimensional phase diagram for the $(La_{1-x}Ca_x)_{1-z}Mn_{1-y}O_{3-\delta}$ system. ■, samples with $x = n_h$, which correspond to Schiffer-like representation;[3] ●, samples with $n_h \cong 0.28$ (O series); ▲, samples with $n_h = 0.50$; ★, samples with $x = 0.50$. The projection on the $n_h - x$ plane is shown at the bottom.

Beyond $x = 0.25$, the data from Table 1 suggest that Ca ions play a substantial role in the setting up of the FM-metallic (uncorrelated) vs the PM (or AF)-insulator phases. This is fully consistent with our model in which the concentration of Ca ions, x, controls the relative ratios of correlated and uncorrelated Ca ions. For FM-C behavior, eq 3, ensuring percolation between Ca ions, must be supplemented by a second requirement, that is, that the uncorrelated regions are connected. The threshold for connectivity in a simple cubic structure (corresponding to the cationic sites) is obtained from standard work in structures with uncorrelated percolation[15] as 0.31. As the size of the uncorrelated volume in our sample is $1 - 2x_1$, we reach a connectivity threshold at

$$1 - 2x_1 = 1 - 2Cx^3 > 0.31 \qquad (4)$$

Using eqs 3 and 4, and substituting eq 3 for q_2, one obtains for metallic-like conductivity and ferromagnetism the condition

$$0.16 < x < 0.45 \qquad (5)$$

which is in excellent agreement with the experimental data of Table 1.

It follows from the preceding discussion that, to understand, reproduce, and even tailor the properties of these manganese perovskites, it is mandatory that x and n_h are independently controlled. Accordingly, data should always be analyzed in three-dimensional phase-diagram plots, an example of which is shown in Figure 2. Examination of this figure shows that, in a three-dimensional diagram, the PM-FM transition temperature corresponds to an extended area (depicted in brown) when n_h and x can be independently modified. Two-dimensional diagrams, such as the one proposed by Schiffer et al.,[4] explore specific planes in that representation such as the diagonal plane indicated in Figure 2.

CM0343599

(15) Stauffer, D. *Phys. Rep.* **1979**, *54* (1), 1.